Free Radical Research, February 2007; 41(2):145–152

informa
healthcare

Postanoxic damage of microglial cells is mediated by xanthine oxidase and cyclooxygenase

REBECCA WIDMER, MARTINA ENGELS, PETER VOSS, & TILMAN GRUNE

Research Institute of Environmental Medicine, Heinrich Heine University, Düsseldorf, Germany

Accepted by Dr J. Keller

(Received 18 May 2006; in revised form 9 August 2006)

Abstract

Brain ischemia and the following reperfusion are important causes for brain damage and leading causes of brain morbidity and human mortality. Numerous observations exist describing the neuronal damage during ischemia/reperfusion, but the outcome of such conditions towards glial cells still remains to be elucidated.

Microglia are resident macrophages in the brain. In this study, we investigated the anoxia/reoxygenation caused damage to a microglial cell line via determination of energy metabolism, free radical production by dichlorofluorescein fluorescence and nitric oxide production by Griess reagent. Consequences of oxidant production were determined by measurements of protein oxidation and lipid peroxidation, as well. By using site-specific antioxidants and inhibitors of various oxidant-producing pathways, we identified major sources of free radical production in the postanoxic microglial cells. The protective influences of these compounds were tested by measurements of cell viability and apoptosis. Although, numerous free radical generating systems may contribute to the postanoxic microglial cell damage, the xanthine oxidase- and the cyclooxygenase-mediated oxidant production seems to be of major importance.

Keywords: *Ischemia, reperfusion, macrophages, microglia*

Abbreviations: *Dpi, diphenylene iodoniumchloride; Ind, Indomethacin; L-Na, L-NAME (*N*-nitro-L-arginine methyl ester); MDA, Malondialdehyde; MQ, MitoQ; Oxy, Oxypurinol; ROS, Reactive oxygen species*

Introduction

Cerebral ischemia, with disruption of blood flow in brain areas, is associated with severe brain damage. It is firmly established that the following reperfusion causes an enhanced free radical production [1,2]. Among the main targets of free radicals are proteins and polyunsaturated fatty acids [3,4], which are highly abundant in the brain, and which will be converted to numerous products, including protein carbonyls and malondialdehyde (MDA). A variety of studies exist about ROS-induced brain injury and oxidative damage after global or focal cerebral ischemia [4–6]. However, an increasing number of relevant reports indicate a pivotal role of microglia in cerebral brain damage [7–9]. Microglial cells derive from the monocyte/macrophage lineage and are highly present in the CNS [10–12]. *In vitro*, these cells are phagocytotic and display class II antigens as response to stimulation [10–13]. They are often exposed to free radicals, since they produce the respiratory burst as pro-inflammatory response. A major mediator for this ROS production is the NADPH oxidase [14]. Furthermore, microglia contain the nitrite oxide synthase isoform NOS-2, which produces NO following calmodulin binding [15–17]. It was also reported that micoglial NO and oxidant production

Correspondence: T. Grune, Research Institute of Environmental Medicine, Heinrich Heine University Düsseldorf, Auf'm Hennekamp 50, 40225 Düsseldorf, Germany. Tel: +49 211 3389 297. Fax: +49 211 3389 226. E-mail: tilman.grune@uni-duesseldorf.de

ISSN 1071-5762 print/ISSN 1029-2470 online © 2007 Informa UK Ltd.
DOI: 10.1080/10715760600978807

might mediate neuronal cell death in neurodegenerative diseases [15]. Besides the NADPH oxidase, other prominent sources of oxidants are the purine- and arachidonic acid metabolism pathways [18–20]. Herein, the enzymes xanthine oxidase and the cyclooxygenases, respectively, are the major players responsible for oxidant production. Furthermore, one of the most important locations of ROS formation is the mitochondrial respiratory chain [21].

Since the ischemic/reperfusion damage in microglial cells was not investigated throughout, we explored in the present study the microglial cell line BV-2 in an anoxia/reoxygenation model. We used several enzyme inhibitors and site-directed antioxidants to evaluate the contribution of several pathways to the postanoxic ROS production.

Material and methods

Cell culture

The mouse microglial cell line BV-2 was cultivated in glutamine-free DMEM, high glucose, supplemented with 1% glutamine, 1% penicilline/streptomycine and 10% bovine calf serum at 37°C and 5% CO_2 in a humidified atmosphere. The cells were seeded in T75 flasks, grown for 2–3 days until sub-confluency and re-cultivated. For experiments, cells were seeded at a density of 6×10^4 cells $\times$ cm^{-2} and harvested by scraping.

Anoxia/reoxygenation

To simulate ischemic conditions, the cells were exposed to anoxic conditions in an anoxic chamber (IUL Instruments GmbH, Königswinter, 37°C, humid atmosphere) in PBS (PAA Austria). PBS was degassed and exposed to anoxic conditions overnight to remove traces of O_2. Normoxic controls were incubated under air in 10 mM glucose in PBS (37°C, humid atmosphere). Reoxygenation was performed by transfer of the anoxic cells to normal (normoxic) conditions in a CO_2 incubator. The PBS was removed and the cells were cultivated in complete medium (DMEM high glucose).

Enzyme inhibitors and antioxidants

Various enzyme inhibitors and antioxidants were used. The compounds were added to the reoxygenation medium before exposure to the cells. Cells were then incubated as described above. The following enzyme inhibitors and antioxidants were applied:

Oxypurinol (Oxy; 10 μM, inhibitor of the xanthine oxidase); indomethacin (Ind; 10 μM, inhibitor of the cyclooxygenases 1 and 2); *N*-nitro-L-arginine methyl ester (L-NAME; 100 μM, inhibitor of the NO-synthase); diphenylene iodoniumchloride (DPI; 20 μM, inhibitor of the NADPH oxidoreductase); MitoQ (10-(6′-ubiquinonyl)decyltriphenylphosphonium, 10 μM, a mitochondria-targeted antioxidant—this compound was kindly provided by Michael Murphy, New Zealand); Trolox (6-hydroxy-2,5,7,8-tetramethylchroman-2-carboxylic acid, 1 mM, an antioxidative water-soluble vitamin E analog).

Determination of cell viability

The Trypan Blue exclusion assay was carried out to test the cell viability by using 0.4% Trypan Blue solution. Cells were scraped and counted in a Fuchs–Rosenthal cell counting chamber. Anoxic cells were harvested under anoxic conditions. Control and reoxygenated cells were handled as usual. Living cells were calculated as percentage to the total cell number.

Apoptosis/caspase-3 assay

Cells were washed once in cold PBS, suspended in cold PBS and counted by the Trypane Blue exclusion method. Cells (1×10^6 cells/ml) were transferred into a lysis buffer provided by BD Biosciences (Pharmingen, Germany). The fluorogenic substrate Ac-DEVD-AMC (5 μl, BD Biosciences) was added to each well/reaction of a 96-well plate containing 200 μl HEPES buffer. The reaction was performed for 1 h at 37°C. The liberated AMC was quantified by spectrofluorometric measurements (Excitation: 380 nm, Emission: 460 nm).

ATP measurements

Cells were suspended in PBS. An equal volume of 6% v/v $HClO_4$ was added to disrupt cells and precipitate the proteins. After short centrifugation (14,000 rpm at 4°C), K_2CO_3 was added to neutralize the acidic solution, and the samples were incubated on ice for 1 h, centrifuged again and stored at −20°C until measurement. The samples were analyzed on an isocratic ion-pair RP-HPLC (column: Supelcosil® 150 × 4.6 mm LC-18-S; 5 μm) using tetrabutylammonium phosphate buffer/acetonitrile eluent. The detection was performed by UV light (254 nm). The adenylate energy charge was calculated as follows: $\{[ATP] + 0.5[ADP]\}/\{[ATP] + [ADP] + [AMP]\}$. The sum of adenylates was calculated as $\{[ATP] + [ADP] + [AMP]\}$.

Measurement of oxidant production

Cellular oxidant production was determined by using the DCFH-DA assay. In brief, cells were incubated with 25 μM DCF-DA (dichlorofluorescein diacetate, Sigma Deisenhofen) in culture medium without fetal calf serum for 45 min at 37°C. DCF-DA is a membrane permeable compound which is hydrolyzed

by intracellular esterases and converted to the fluorescent dichlorofluorescin (DCF) when oxidized. After DCF-DA loading, the cells were washed twice with warm PBS and subjected to anoxia/reoxygenation. The fluorescence was measured in a fluorimeter at an excitation wavelength of 485 nm and an emission wavelength of 538 nm at the indicated time-points.

Measurement of NO formation

The NO production was assessed by the Griess test. In brief, culture supernatant was mixed with an equal volume of Griess reagent (Sigma). The absorbance was measured within 10 min in a plate reader at 540 nm.

Protein oxidation measurements

Protein carbonyls were measured by using the method of Buss et al. [22], modified by Sitte et al. [23]. Samples of cell lysates were derivatized with 2,4-dinitrophenylhydrazine and adsorbed to Maxisorb multiwell plates (Nunc, Germany). Protein carbonyls were detected using an anti-DNP primary antibody and an anti-rabbit-IgG peroxidase linked secondary antibody. *O*-phenyl diamine was used to develop the plate and the absorbance was determined using a multiwell plate reader and a detection wavelength of 492 nm.

Lipid peroxidation measurements

MDA was determined by the method of Wong et al. [24], with modifications of Sommerburg et al. [25]. After addition of thiobarbituric acid, the cell suspensions (lysates) were boiled for 1 h. Cooling the samples on ice stopped the reaction. The samples were neutralized with NaOH and analyzed on an isocratic RP-HPLC (column: Supelcosil® 150 × 4 mm LC-18-S; 5 μm) using a potassium phosphate buffer/methanol eluent. The detection was performed by fluorescence (excitation: 525 nm/emission: 550 nm).

Statistical analysis

Data are represented as mean ± SEM and were analyzed by using the Student's *t*-test after testing for a normal distribution. Significance was assumed at the $p < 0.05$ level of confidence.

Results

In order to mimic the physiological conditions of ischemia, we used an approach known as oxygen–glucose-depletion common in brain ischemia research. Such a condition is adding to the anoxia also a loss of extracellular energy substrates as glucose, fatty acids or amino acids. Therefore, BV-2 cells were washed and placed in PBS without oxygen. The viability of BV-2 cells under such conditions was tested for up to 16 h. We found a decrease in viability with time (Figure 1A). After 6 h incubation some 55% of the cells are still able to exclude Trypan Blue. A further increase of the anoxic period is accompanied by a dropping of this percentage. We chose the 6 h anoxic period in order to perform reoxygenation experiments. BV-2 cells were transferred to normoxic (20% oxygen) conditions together with the exposure to fresh tissue culture medium (containing all substrates). These conditions reflect best the *in vivo* conditions of reperfusion. During reoxygenation the ability of cells to exclude Trypan Blue increased to above 70% after 18 or 24 h (Figure 1B).

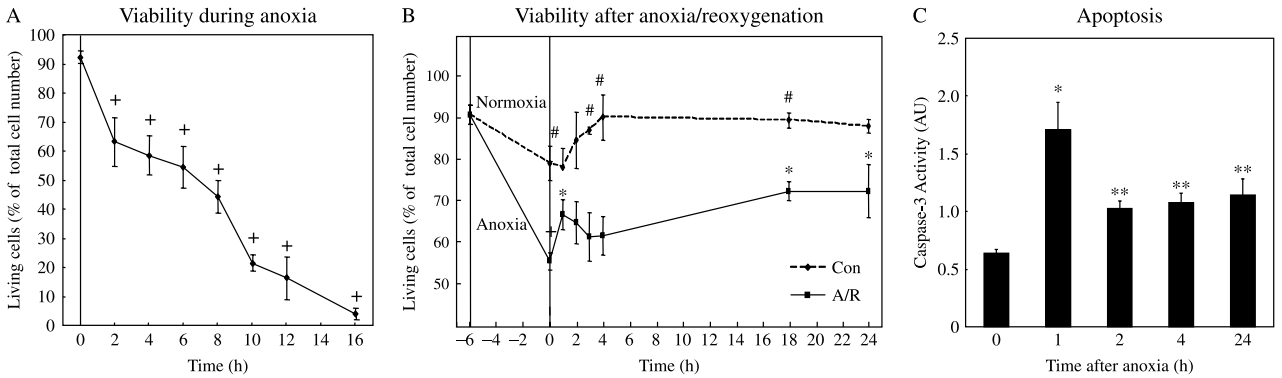

Figure 1. Viability during anoxia/reoxygeneation of BV-2 cells. Viability was tested by Trypan Blue exclusion test (Panel A and B) as described in the methods section. The decrease of viability during anoxia is presented in Panel A. Panel B demonstrates the viability during the reoxygenation after a 6 h anoxic period (A/R = anoxia/reoxygenation). The normoxic control (Con) was exposed for 6 h to PBS with 10 mM glucose (under the normal oxygenating conditions) and afterwards to normal tissue culture medium. Apoptosis was analyzed by determination of caspase-3 activity by using the fluorogenic substrate Ac-DEVD-AMC (Panel C). The fluorescence of normoxic, untreated cells was set as 1. Time point 0 indicates the start of reoxygenation. The data represent the mean ± SEM of six independent experiments in Figure 1A and 1B, and the mean ± SEM of four independent experiments in Figure 1C. Statistical significance symbols indicate: $+p < 0.05$ before anoxia vs. various time points of anoxia, $*p < 0.05$ after anoxia (0 h) vs. various time points of reoxygenation, $**p < 0.05$ indicated column vs. 1 h of reoxygenation, $\#p < 0.05$ control (normoxia) vs. various time points of reoxygenation.

To elucidate whether apoptosis plays a critical role in the loss of viability, we tested the activity of caspase-3 since this is one of the main mediators induced within both, the deathreceptor dependent (extrinsic) and the death-receptor independent (intrinsic) apoptotic pathways. We found a 30% decrease after 6 h anoxia compared to normoxic caspase-3 activity levels. This is in concert with the fact that apoptosis, as far as the intrinsic apoptotic pathway is concerned, is an ATP-dependent (mitochondria-dependent) process. Once, ATP production was re-established due to the reoxygenation conditions, the apoptosis rate was enhanced (Figure 1C). There were no detectable changes in the apoptosis rates in the normoxic control over time.

To check, whether the oxygen and substrate deprivation really leads to a drastic decline in the cellular ATP level we performed HPLC analysis of the ATP and ADP levels. As demonstrated in Figure 2A, a drastic decline of ATP concentrations takes place during the 6 h of anoxia. The ATP levels are recovering within the first hour of reoxygenation. Interestingly, the quick recovery of the ATP level is accompanied by a drop of the ADP level, resulting in a postanoxic ATP/ADP ratio higher as the normoxic control (Figure 2B). These changes were accompanied by changes in the adenylate energy charge from a normoxic value of 0.74 ± 0.06 to 0.51 ± 0.04 during anoxia and 0.79 ± 0.07 after 1 h of reoxygenation (mean $\pm$ SE, $n = 4$). Interestingly, the sum of adenylates was not changing during anoxia 34.6 ± 5.7 nmol $\times$ mg protein^{-1} (vs. $35.2 + 7.1$ nmol $\times$ mg protein^{-1} in normoxia), but dropped after 1 h of reoxygenation to 25.4 ± 5.1 nmol $\times$ mg protein^{-1} (mean $\pm$ SE, $n = 4$). There were no detectable changes in the adenine nucleotide levels in the normoxic control over time.

Since the loss of energy is quickly overcome by BV-2 cells in the postanoxic phase, the major reason for the inability of cells to recover viability might be the postanoxic production of free radicals or oxidants leading to cellular damage and apoptosis. Therefore, we decided to measure various oxidative stress related parameters and started with the production of DCFH-DA oxidizing species. The fluorogenic compound DCFH-DA is one of the most prominent markers to reflect the overall oxidative status in cells [26]. DCF-DA is reported to be oxidized by a variety of ROS like hydrogen peroxide, organic hydroperoxides, nitric oxide and peroxynitrite [27–29]. As shown in Figure 3A, a dramatic increase in DCF fluorescence takes place after 2 h postanoxic incubation. This increase is significant towards the end of anoxia as well as towards the time-matched normoxic control (Figure 3A, insert). The normoxic control levels of DCF fluorescence were in the range of 100–130% (data not shown). Since it is well known that microglial cells produce NO in high quantities due to the inducible NO-synthase, we assessed the NO-production by exploring the Griess reagent. As demonstrated in Figure 3B, the Griess reagent reaction is clearly enhanced after 1 h reoxygenation.

To measure the consequences of enhanced oxidant production, we determined actual damage parameters as protein oxidation- and lipid peroxidation-products. It is highly established that proteins, which are abundant and ubiquitous in the cell, are able to form protein carbonyls as response to direct oxidative stress [30,31]. A significant increase in protein carbonyls could be observed after 1 h reoxygenation (Figure 3C). On the other hand, a multitude of lipid peroxidation products are generated during oxidative stress. Among the aldehydic lipid peroxidation products, malondialdehyde is an easy one to measure. We were able to find an increase in the malondialdehyde concentration only 24 h after the beginning of the reoxygenation (Figure 3D). However, the failure to measure some earlier increase in this product might be due to the

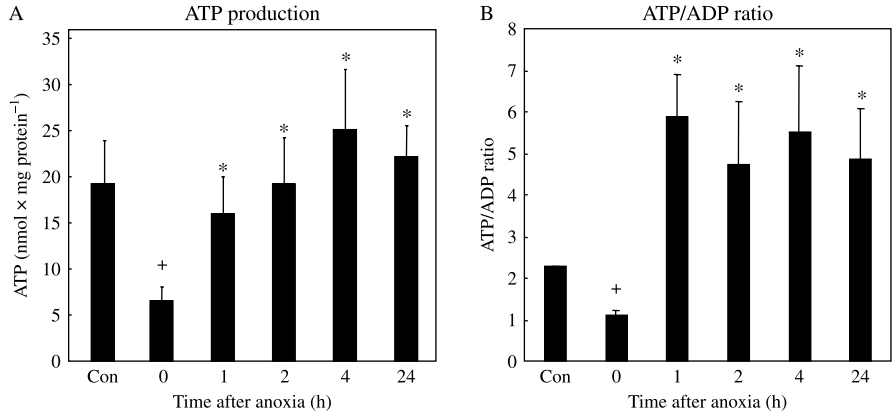

Figure 2. ATP content and ATP/ADP in anoxic and postanoxic BV-2 cells. Anoxia/reoxygenation was performed as described above. ATP and ADP were determined by HPLC analysis. The ATP content (Panel A) and the ATP/ADP-ratio (Panel B) were measured before anoxia (Con) after 6 h of anoxia (0 h) and at the indicated reoxygenation times. The data represent the mean $\pm$ SEM of 4 independent experiments; $+p < 0.05$ control (normoxia) vs. 6 h anoxia (0 h), and $*p < 0.05$ after anoxia (0 h) vs. various times of reoxygenation.

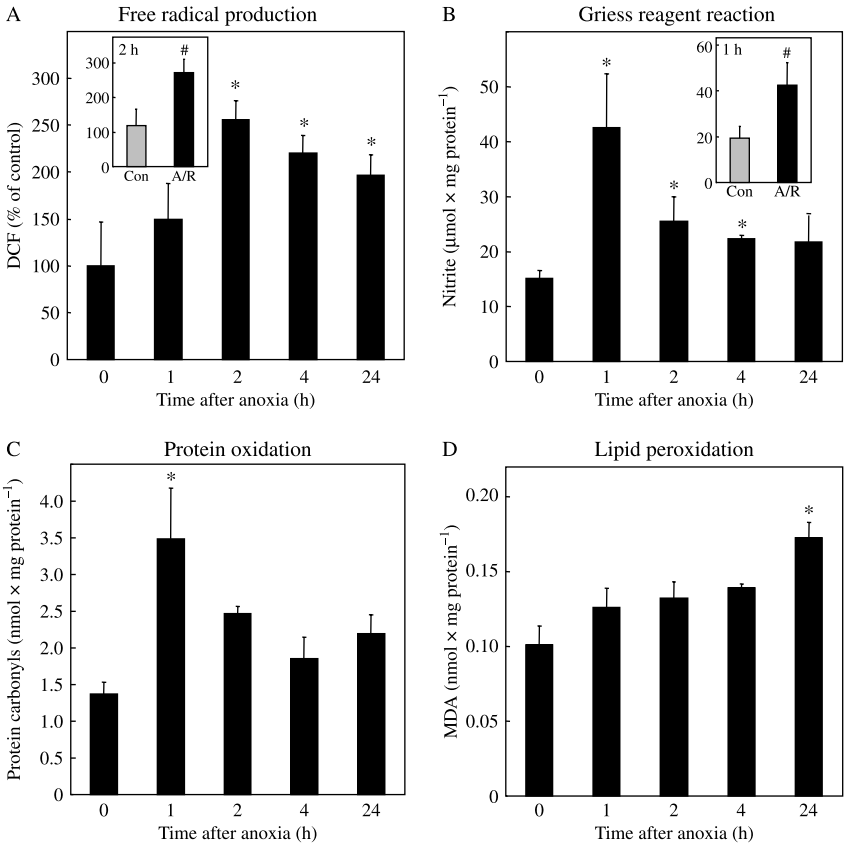

Figure 3. Oxidant production, protein oxidation and lipid peroxidation in postanoxic BV-2 cells. Experiments were performed as described in the methods section. The determination of reactive oxygen species was performed by employment of the DCF-DA assay (Panel A). The fluorescence level directly after anoxia was set as 100%. The insert shows the comparison of the postanixic fluorescence (A/R) and the normoxic control (Con) at the 2 h time point. The data represent the mean ± SEM of three independent experiments; $\star p < 0.05$ anoxia reoxygenation (0 h) vs. various times of reoxygenation and # anoxia/reoxygenation vs. time matched control. The measurement of Griess reagent reactive products is shown in Panel B. The data represent the mean ± SEM of three independent experiments; $\star p < 0.05$ after anoxia (0 h) vs. various times of reoxygenation. The insert shows the normoxic control level (Con) in comparison to the postanoxic level (A/R) at 1 h of reoxygenation. $\star p < 0.05$ #anoxia/reoxygenation vs. time matched control. Panel C demonstrates the protein carbonyl formation measured by the ELISA method described in the methods section, whereas Panel D is showing the formation of malondialdehyde determined by HPLC. The data represent the mean ± SEM of three independent experiments; $\star p < 0.05$ after anoxia (0 h) vs. reoxygenation.

rapid metabolism described for aldehydic lipid peroxidation products.

In the next series of experiments, we tested for the source of the oxidative stress in the postanoxic BV-2 cells. Here, we measured protein oxidation and lipid peroxidation in the presence of various antioxidants and inhibitors. As demonstrated in Figure 4, all used compounds had a dramatic effect on the protein carbonyl formation. On the other hand, only oxypurinol and indomethacin were able to suppress lipid peroxidation. This leads to the speculation that the increase of protein carbonyls in BV-2 cells is a rather complex process mediated by a network of oxidative processes, whereas the maintenance of the lipid hydroperoxide levels (measured by malondialdehyde) is mediated by xanthine oxidase and cyclooxygenases. To test the role of these inhibitors on the cell viability and apoptosis induction, we performed the required measurements in the presence of the inhibitors. As demonstrated in Figure 5A, only oxypurinol and indomethacin lead to a notable increase in cell viability 1 h after anoxia. On the other hand, no significant decline in caspase-3 activation could be detected using the inhibitors. However, the antioxidants MitoQ and Trolox suppress the postanoxic caspase-3 activation significantly without increasing Trypan Blue exclusion.

Discussion

Little is known about postanoxic microglial damage and ROS production. Therefore, we measured the postanoxic radical formation and their potential sources. Our study is contributing to the hypothesis that besides cell types like neurons and capillary endothelial cells, microglia are highly involved in cerebral tissue damage during ischemia/reperfusion due to their ability to produce ROS. The viability of BV-2 cells under hypoxic conditions was dramatically declining, whereas no Caspase 3 activation could be determined. On the other hand, during reoxygenation a "recovery" of Trypan blue-measured viability was

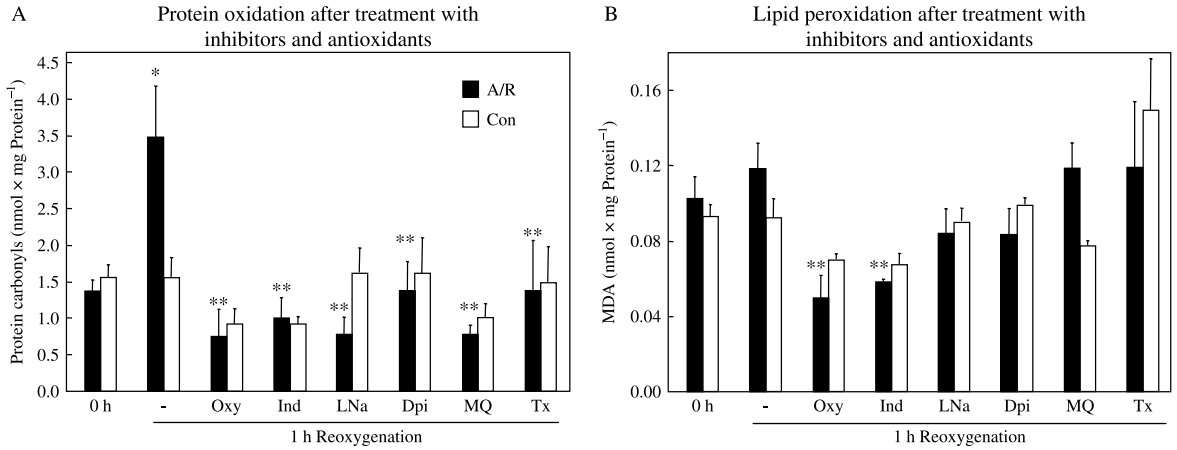

Figure 4. Effects of enzyme inhibitors and antioxidants on postanoxic protein oxidation and lipid peroxidation. Various enzyme inhibitors and antioxidants were used to test the effect of free radical generating pathways on the postanoxic damage in BV-2 cells (for conditions and concentrations see methods section). Panel A demonstrates the effect of these compounds on protein oxidation, whereas Panel B demonstrates the effects on malondialdehyde formation. The filled bars show the data from anoxia/reoxygenation experiments (A/R), whereas the open columns represent the normoxic control (Con). All measurements were performed at 1 h of reoxygenation with the exception of the postanoxic measurements (0 h), which were done directly after the 6 h of anoxia. The data represent the mean ± SEM of three independent experiments. Statistical evaluation is performed within the anoxia/reoxygenation group: $\star p < 0.05$ after anoxia (0 h) vs. 1 h reoxygenation, and $\star\star p < 0.05$ 1 h reoxygenation nontreated vs. treated.

determined, whereas Caspase 3 was activated to a certain degree. The key factor in the explanation of this seems to be the presence of ATP. Under anoxic conditions cells seem not have sufficient ATP to perform a full-scale apoptotic process and to exclude Trypan blue. During reoxygenation some cells re-synthesize ATP and whereas other cells go into apoptosis.

It was assumed that NADPH oxidase and/or NO-synthase are the major causes for ROS production. NADPH oxidase- and NO-synthase activity is activated in microglia during ischemia/reperfusion [8,32–35]. Ischemia-induced overproduction of NO is caused by glutamate-mediated increases in intracellular calcium concentrations, resulting in a calmodulin-dependent up-regulation of NO-synthase [33–36]. However, both of these enzymes do not seem to be the major oxidant sources in the postanoxic microglial cell. The most prominent enzymes responsible for oxidative microglial damage seem to be the xanthine oxidase and cyclooxygenases. Postanoxic xanthine oxidase formation is also triggered by calcium [18]. The protease calpain, activated by elevated calcium levels, cleaves the xanthine dehydrogenase to form xanthine oxidase [37,38]. In contrast to the dehydrogenase form, which is only able to reduce NAD^+, the oxidase form can use molecular oxygen to produce highly reactive superoxide or hydrogen peroxide [18]. Concomitantly, during ischemia, ATP is depleted to AMP. AMP is further metabolized to

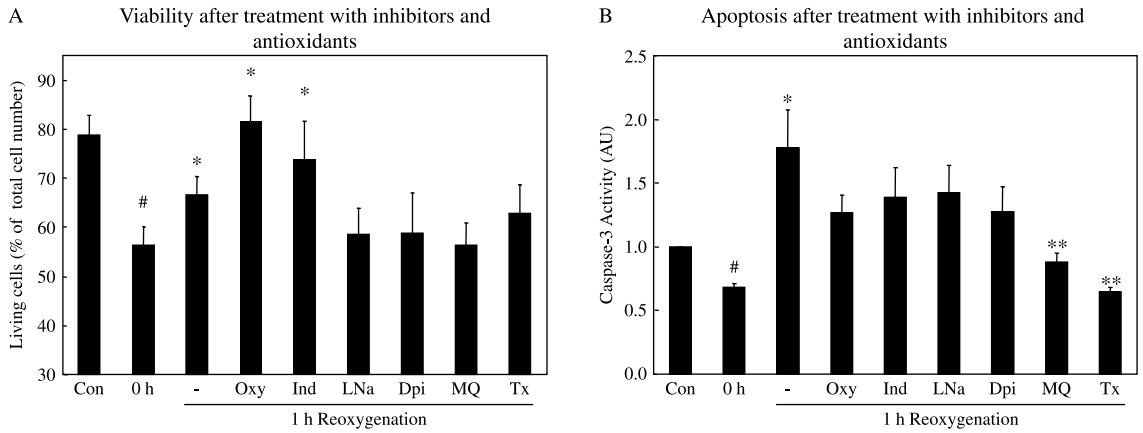

Figure 5. Effect of enzyme inhibitors and antioxidants on postanoxic cell viability. Experiments were performed as described above. Viability (Panel A) and apoptosis (Panel B) were measured via Trypan Blue exclusion test and caspase-3-activity, respectively. The data represent the mean ± SEM of 4–6 independent experiments; $\star p < 0.05$ indicated column vs. anoxia (0 h), $\star\star p < 0.05$ indicated column vs. 1 h reoxygenation without treatment.

hypoxanthine, which, as well as xanthine, can be oxidized by xanthine dehydrogenase or xanthine oxidase [18]. Cyclooxygenases 1 and 2 (COX-1 and COX-2) are the rate-limiting enzymes for prostaglandin and thromboxane biosynthesis. COX-1 is the constitutively expressed isoform, whereas COX-2 is induced in response to endotoxin, inflammatory cytokines and growth factors [39,40]. The expression of COX-2 is transiently triggered by focal cerebral ischemia [41–44] or after forebrain ischemia [45]. Furthermore, it has been shown that microglia is the major source of prostaglandin production after chronic cerebral ischemia [7].

Concluding, the results described in this study are suggestive that the xanthine oxidase and cyclooxygenases play a major role in microglial ROS production in postanoxic situations. Other sources also contribute to the postanoxic oxidative stress with no apparent influence on Trypan Blue exclusion.

Acknowledgements

This study was supported by DFG and BMU. We thank Prof. Michael Murphy, New Zealand for the kind gift of MitoQ.

References

[1] Kontos CD, Wei EP, Williams JI, Kontos HA, Povlishock JT. Cytochemical detection of superoxide in cerebral inflammation and ischemia *in vivo*. Am J Physiol 1992;263:H1234–H1242.

[2] Dirnagl U, Lindauer U, Them A, Schreiber S, Pfister HW, Koedel U, Reszka R, Freyer D, Villringer A. Global cerebral ischemia in the rat: Online monitoring of oxygen free radical production using chemiluminescence *in vivo*. J Cereb Blood Flow Metab 1995;15:929–940.

[3] Chan PH. Reactive oxygen radicals in signaling and damage in the ischemic brain. J Cereb Blood Flow Metab 2001;21:2–14.

[4] Chan PH. Oxygen radicals in focal cerebral ischemia. Brain Pathol 1994;4(1):59–65.

[5] Kontos HA, George E. Brown memorial lecture. Oxygen radicals in cerebral vascular injury. Circ Res 1985;57:508–516.

[6] Siesjo BK, Agardh CD, Bengtsson F. Free radicals and brain damage. Cerebrovasc Brain Metab Rev 1989;1:165–211.

[7] Tomimoto H, Akiguchi I, Wakita H, Lin JX, Budka H. Cyclooxygenase-2 is induced in microglia during chronic cerebral ischemia in humans. Acta Neuropathol (Berl) 2000; 99:26–30.

[8] Spranger M, Kiprianova I, Krempien S, Schwab S. Reperfusion increases the release of reactive oxygen intermediates in murine microglia. J Cereb Blood Flow Metab 1998;18:670–674.

[9] Gibson CL, Coughlan TC, Murphy SP. Glial nitric oxide and ischemia. Glia 2005;50:417–426.

[10] Hickey WF, Kimura H. Perivascular microglial cells of the CNS are bone marrowderived and present antigen *in vivo*. Science 1988;239:290–292.

[11] Perry VH, Gordon S. Macrophages and microglia in the nervous system. Trends Neurosci 1988;11:273–277.

[12] Streit WJ, Graeber MB, Kreutzberg GW. Functional plasticity of microglia: A review. Glia 1988;1:301–307.

[13] Frei K, Siepl C, Groscurth P, Bodmer S, Schwerdel C, Fontana A. Antigen presentation and tumor cytotoxicity by interferon-gamma-treated microglial cells. Eur J Immunol 1987;17:1271–1278.

[14] Rosen GM, Pou S, Ramos CL, Cohen MS, Britigan BE. Free radicals and phagocytic cells. FASEB J 1995;9:200–209.

[15] Boje KM, Arora PK. Microglial-produced nitric oxide and reactive nitrogen oxides mediate neuronal cell death. Brain Res 1992;587:250–256.

[16] Chao CC, Hu S, Molitor TW, Shaskan EG, Peterson PK. Activated microglia mediate neuronal cell injury via a nitric oxide mechanism. J Immunol 1992;149:2736–2741.

[17] Zielasek J, Tausch M, Toyka KV, Hartung HP. Production of nitrite by neonatal rat microglial cells/brain macrophages. Cell Immunol 1992;141:111–120.

[18] McCord JM. Oxygen-derived free radicals in postischemic tissue injury. N Engl J Med 1985;312:159–163.

[19] Akundi RS, Candelario-Jalil E, Hess S, Hull M, Lieb K, Gebicke-Haerter PJ, Fiebich BL. Signal transduction pathways regulating cyclooxygenase-2 in lipopolysaccharide activated primary rat microglia. Glia 2005;51:199–208.

[20] Sairanen T, Ristimaki A, Karjalainen-Lindsberg ML, Paetau A, Kaste M, Lindsberg PJ. Cyclooxygenase-2 is induced globally in infracted human brain. Ann Neurol 1998;43:738–747.

[21] Turrens JF. Mitochondrial formation of reactive oxygen species. J Physiol 2003;552:335–344.

[22] Buss H, Chan TP, Sluis KB, Domigan NM, Winterbourn CC. Protein carbonyl measurement by a sensitive ELISA method. Free Radic Biol Med 1997;23:361–366.

[23] Sitte N, Merker K, Grune T. Proteasome-dependent degradation of oxidized proteins in MRC-5 fibtroblasts. FEBS Lett 1998;440:399–402.

[24] Wong SH, Knight JA, Hopfer SM, Zaharia O, Leach CN Jr, Sunderman FW Jr. Lipoperoxides in plasma as measured by liquid-chromatographic separation of malondialdehyde–thiobarbituric acid adduct. Clin Chem 1987;33:214–220.

[25] Sommerburg O, Grune T, Klee S, Ungemach FR, Siems WG. Formation of 4-hydroxynonenal and further aldehydic mediators of inflammation during bromotrichlormethane treatment of rat liver cells. Med Inflamm 1993;2:27–31.

[26] Wang H, Joseph JA. Quantifying cellular oxidative stress by dichlorofluorescein assay using microplate reader. Free Radic Biol Med 1999;27:612–616.

[27] Keston AS, Brandt R. The analysis of ultramicro quantities of hydrogen peroxide. Anal Biochem 1965;11:1–5.

[28] Gabriel C, Camins A, Sureda FX, Aquirre L, Escubedo E, Pallas M, Camarasa J. Determination of nitric oxide generation in mammalian neurons using dichlorofluorescin diacetate and flow cytometry. J Pharmacol Toxicol Methods 1997;38:93–98.

[29] Possel H, Noack H, Augustin W, Keilhoff G, Wolf G. 2,7-Dihydrodichlorofluorescein diacetate as a fluorescent marker for peroxynitrite formation. FEBS Lett 1997;416:175–178.

[30] Stadtman ER. Importance of individuality in oxidative stress and aging. Free Radic Biol Med 2002;33:597–604.

[31] Carrard G, Bulteau AL, Petropoulos I, Friguet B. Impairment of proteasome structure and function in aging. Int J Biochem Cell Biol 2002;34:1461–1474.

[32] Gyenes M, De Groot H. Prostanoid release by Kupffer cells upon hypoxia-reperfusion: Role of pHi and Cai^{2+}. Am J Physiol 1993;264:G535–G540.

[33] Dawson VL, Dawson TM, London ED, Bredt DS, Snyder SH. Nitric oxide mediates glutamate neurotoxicity in primary cortical cultures. Proc Natl Acad Sci USA 1991;88:6368–6371.

[34] Garthwaite J, Charles SL, Chess-Williams R. Endothelium-derived relaxing factor release on activation of NMDA receptors suggests role as intercellular messenger in the brain. Nature 1988;336:385–388.

[35] Garthwaite J, Garthwaite G, Palmer RM, Moncada S. NMDA receptor activation induces nitric oxide synthesis from arginine in rat brain slices. Eur J Pharmacol 1989;172:413–416.

[36] Kwon NS, Nathan CF, Gilker C, Griffith OW, Matthews DE, Stuehr DJ. L-citrulline production from L-arginine by macrophage nitric oxide synthase. The ureido oxygen derives from dioxygen. J Biol Chem 1990;265:13442–13445.

[37] Wu S, Tamaki N, Nagashima T, Yamaguchi M. Reactive oxygen species in reperfusion injury of rat brain capillary endothelial cells. Neurosurgery 1998;43:577–583.

[38] Roy RS, McCord JM. Superoxide and ischemia: Conversion of xanthine dehydrogenase to xanthine oxidase. In: Greenwald R, Cohen G, editors. Oxy radicals and their scavenger systems. Vol. 2. Cellular and molecular aspects. New York, NY: Elsevier; 1983. p 143–145.

[39] Elmquist JK, Breder CD, Sherin JE, Scammell TE, Hickey WF, Dewitt D, Saper CBJ. Intravenous lipopolysaccharide induces cyclooxygenase 2-like immunoreactivity in rat brain perivascular microglia and meningeal macrophages. Comp Neurol 1997;381:119–129.

[40] Feng L, Xia Y, Garcia GE, Hwang D, Wilson CB. Involvement of reactive oxygen intermediates in cyclooxygenase-2 expression induced by interleukin-1, tumor necrosis factor-alpha, and lipopolysaccharide. J Clin Invest 1995;95:1669–1675.

[41] Collaco-Moraes Y, Aspey B, Harrison M, de Belleroche J. Cyclo-oxygenase-2 messenger RNA induction in focal cerebral ischemia. J Cereb Blood Flow Metab 1996;16:1366–1372.

[42] Miettinen S, Fusco FR, Yrjanheikki J, Keinanen R, Hirvonen T, Roivainen R, Narhi M, Hokfelt T, Koistinaho J. Spreading depression and focal brain ischemia induce cyclooxygenase-2 in cortical neurons through *N*-methyl-D-aspartic acid-receptors and phospholipase A2. Proc Natl Acad Sci USA 1997;94:6500–6505.

[43] Nogawa S, Zhang F, Ross ME, Iadecola C. Cyclo-oxygenase-2 gene expression in neurons contributes to ischemic brain damage. J Neurosci 1997;17:2746–2755.

[44] Sanz O, Estrada A, Ferrer I, Planas AM. Differential cellular distribution and dynamics of HSP70, cyclooxygenase-2, and c-Fos in the rat brain after transient focal ischemia or kainic acid. Neuroscience 1997;80:221–232.

[45] Ohtsuki T, Kitagawa K, Yamagata K, Mandai K, Mabuchi T, Matsushita K, Yanagihara T, Matsumoto M. Induction of cyclooxygenase-2 mRNA in gerbil hippocampal neurons after transient forebrain ischemia. Brain Res 1996;736:353–736.